Supporting Information

Electron mobility of 24 $cm^2\ V^{-1}\ s^{-1}$ in PbSe Colloidal-Quantum-Dot Superlattices

*Daniel M. Balazs, Bartosz M. Matysiak, Jamo Momand, Artem G. Shulga, Maria Ibáñez, Maksym V. Kovalenko, Bart J. Kooi, Maria Antonietta Loi**

E-mail: m.a.loi@rug.nl

Additional figures

Contact resistance and contactless mobility calculation

Ion-gel characterization

Additional figures

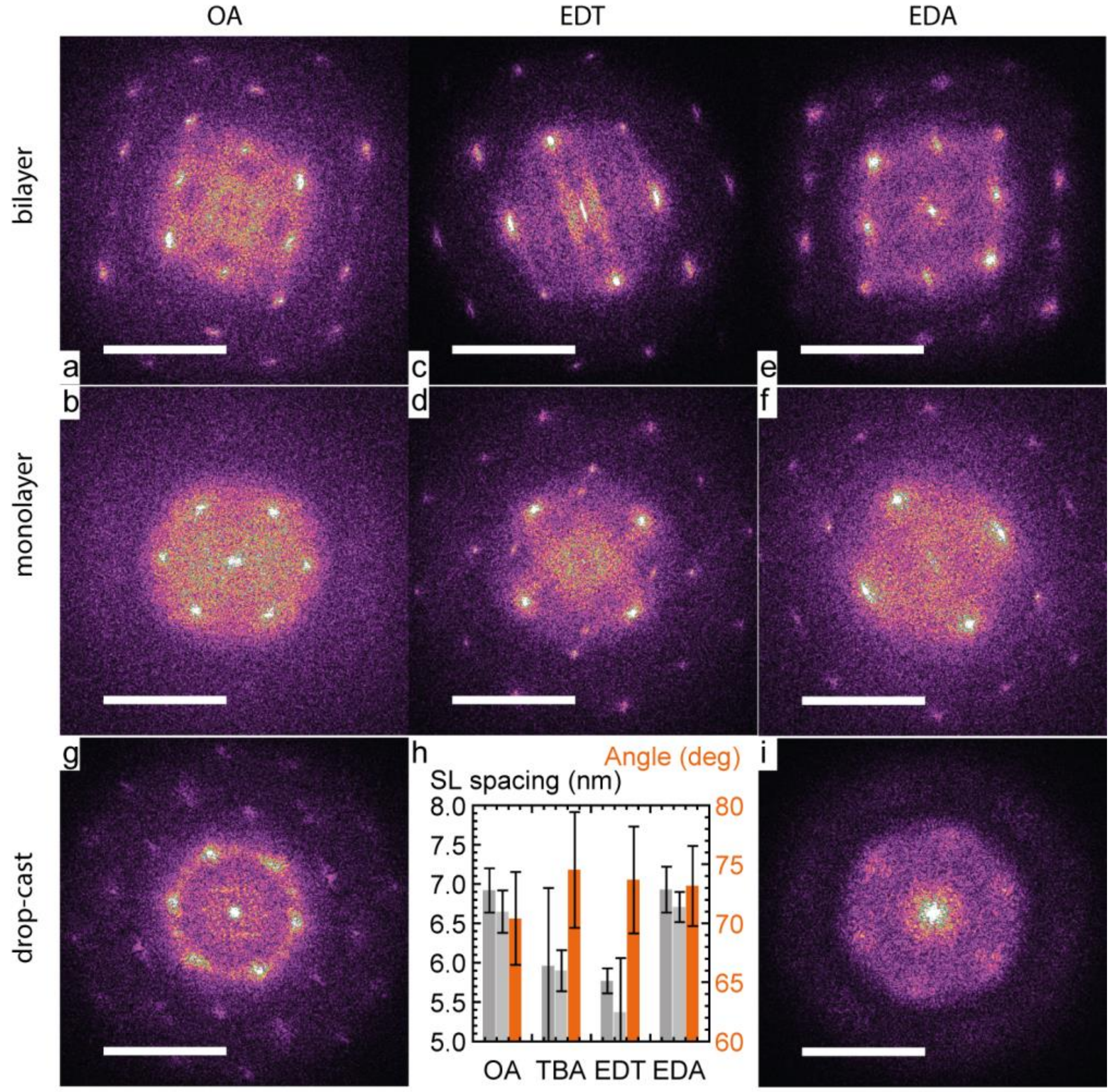

Figure S1. *Fast-Fourier-transformed TEM images of (a,c,e) bilayer and (b,d,f) monolayer superlattices, and (g,i) drop-cast samples using (a,b,g) OA, (c,d) EDT and (e,f,i) EDA ligands, the scale bars are 0.3 nm^{-1}; (h) extracted lattice parameters for bilayer superlattices.*

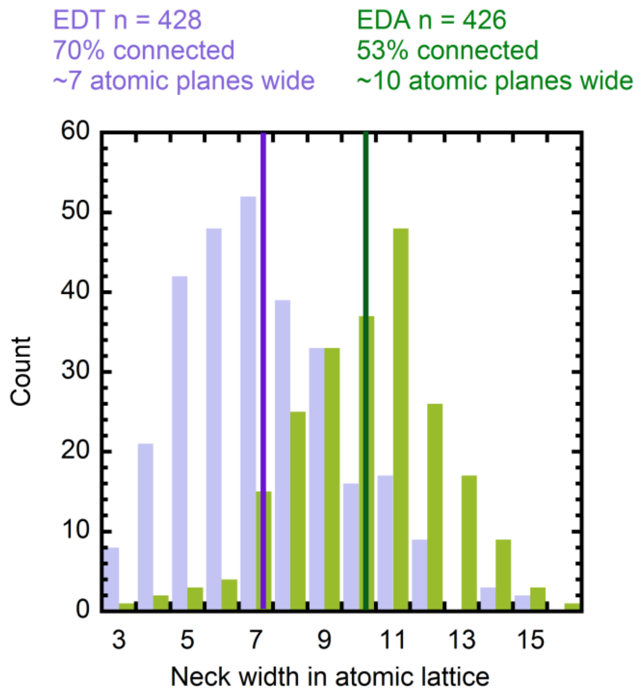

Figure S2. *Quantification of the neck width in EDT- and EDA-treated superlattices, the statistic is reporting more than 400 necks for both samples, the two lines indicate the average of the 2 distributions.*

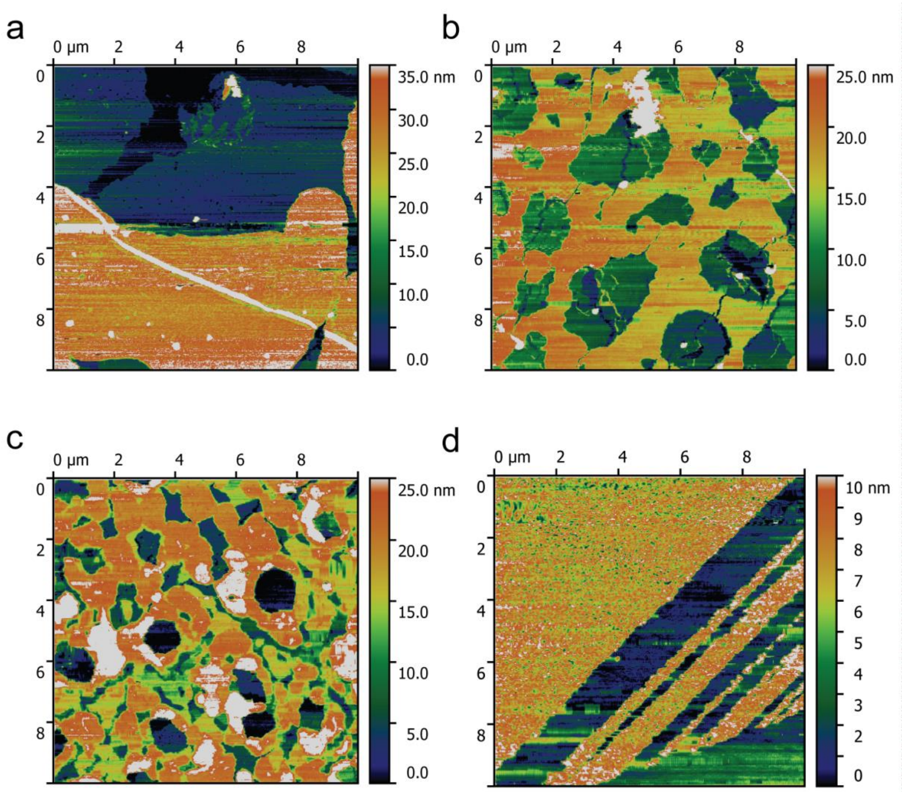

Figure S3. *AFM images of superlattices formed using a) OA, b) EDT and c) EDA ligand, and d) image of the spin-coated reference sample showing a more homogeneous, but granular structure.*

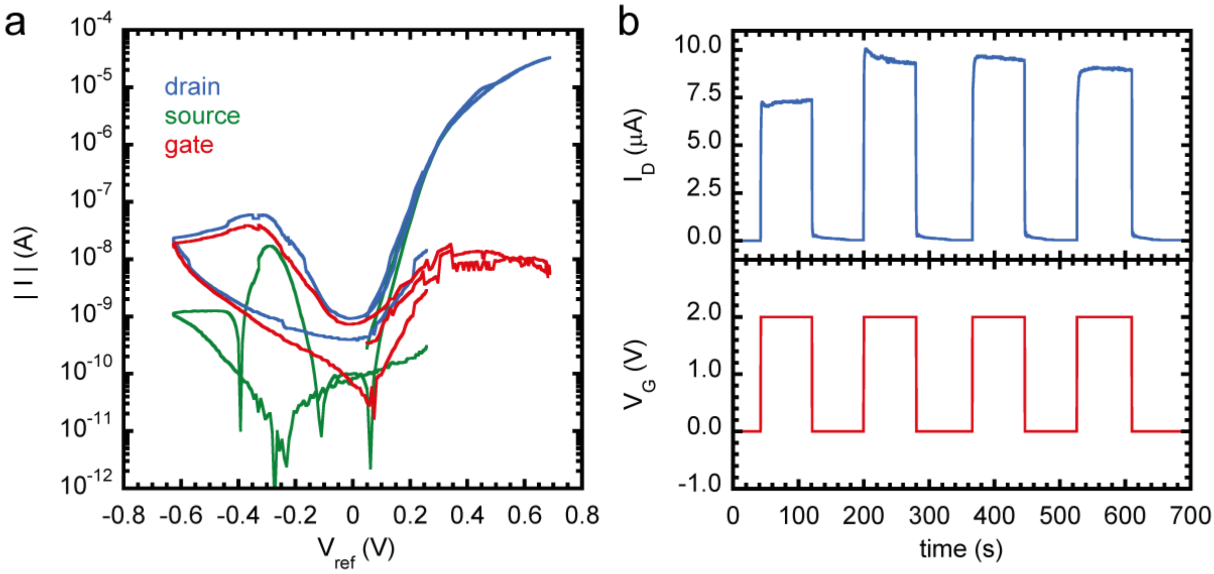

Figure S4. *Additional transport properties: a) typical drain, source and gate currents in a PbSe CQD superlattice IGFET; b) Transient behavior of ion-gel-gated PbSe superlattice FETs: the gate has to be loaded and unloaded to reach stable and reproducible threshold and "on" currents.*

Sample	Substrate #	Area #	Channel length (µm)	Mobility (cm^2/Vs)
SL-EDA	1	1	3	40.4
		2	5	30.6
		3	5	46.2
		4	5	41.5
	2	1	2	10.1
			5	8.09
			10	7.51
		2	2	10.1
			3	14.8
			5	14.0
			10	16.4
	3	1	2	16.7
			3	13.1
			5	19.8
			10	25.2
		2	3	7.24
		3	2	6.95
SP-EDA	1	1	3	3.92
		2	3	2.63
			5	7.92
		3	5	0.84
SL-EDT	1	1	5	2.47
	2	1	3	2.27
			5	5.11
		2	3	6.26
			5	4.21
SL-TBAI	1	1	5	10.9
		2	5	3.12
SL-OA	1	1	5	7.17
		2	3	4.90
			5	8.42
		3	5	2.26

Table S1. *Mobility values calculated from the collected transfer curves, indicating which devices belong to the same substrate and the location.*

Contact resistance analysis

Contact resistances were calculated using the transfer line method. Devices of the same set with several different channel lengths were measured, and the total resistances at the same effective gate voltage $\Delta V = V_g - V_{th}$ were plotted against the channel length. The contact resistance (R_c) is obtained by a linear fit:

$$R_{tot} = R_c + \frac{L}{\mu C W \Delta V} \quad \textbf{(S1)}$$

where L and W are the channel length and width, C is the gate capacitance, and μ is the mobility. The contactless mobility (μ_0) can then be calculated as:

$$\mu_0 = \frac{\partial \left(\frac{\partial R_{tot}}{\partial L}\right)^{-1}}{\partial V_g} \frac{1}{CW} \quad \textbf{(S2)}$$

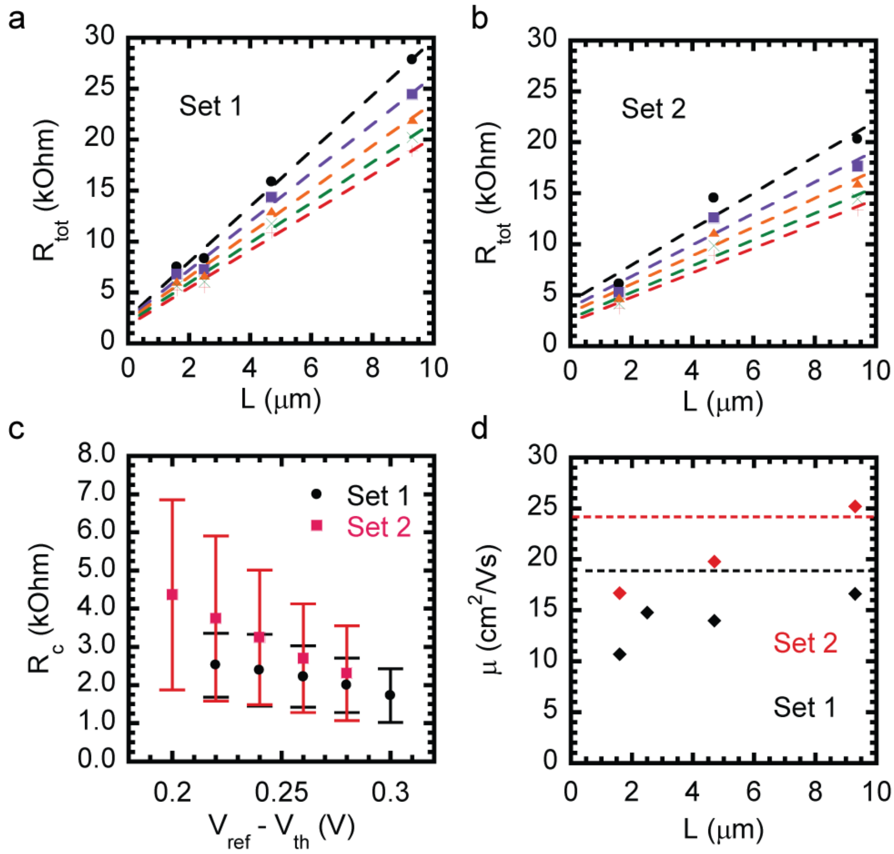

Figure S5. *Transfer line method determination of the contact resistance and contactless mobility in two sets of PbSe superlattice FETs: (a,b) resistance vs channel length in devices in proximity;(c) the resistance decreases with increasing carrier concentration, and is similar in both sets of devices; (d) contactless mobility values (dashed line) 10-80% higher than the raw data (markers) are calculated for the two sets following Equation S2.*

Ion gel capacitance measurements

The capacitance of the ion gel was measured forming larger area capacitors between flat electrode surfaces. Four bottom electrodes were used: ITO, gold, gold with a monolayer of PbSe and gold with the multilayer PbSe used in the research. The substrate/bottom electrode was covered with a droplet of the ion gel, dried the same way as the devices, and a Pt foil electrode was placed on top. In case of the ITO substrate, droplets of several size were formed and in total 5 electrode pairs were characterized. For the gold-based samples, two top electrodes of different size were placed on top of the same droplet. The impedance data between 10 mHz and 100 Hz were fitted with the theoretical expression for a constant phase element (CPE) for each set of data (see Equation S3). To determine the effective capacitance (C_{eff}), the imaginary part of the CPE impedance as a function of frequency was expressed as the impedance of a capacitor, and the values were calculated at 63 mHz frequency, equivalent to the 5 mV/s rate used in the FET measurements) using Equation S4:

$$Z_{CPE} = Qf^{a} * e^{-i\pi a} \quad Z_{C,eff} = Im(Z_{CPE}) \qquad Z_{C,eff} = (i2\pi f C_{eff})^{-1} \qquad \textbf{(S3)}$$

$$C_{eff} = Q(2\pi f)^{a-1}\sin(-\frac{\pi a}{2}) \qquad \textbf{(S4)}$$

Examples for the devices are shown on Figure S6(a-b). The obtained capacitance values are plotted against the effective device area $1/A_{eff} = 1/A_{top} + 1/A_{bottom}$ on Figure S5(c). The slopes were determined by fixing the intercept at 0, and are collected on panel d. The bare gold- and thin PbSe-based samples show very similar slopes around 8 μF/cm^2. The ITO-based capacitors behave very similar to the one prepared the same way as out actual samples, with a slope of 6 μF/cm^2. The slopes are the average electrode capacitance of that system, and the differences can shed light to differences in the electrode surfaces, for example. In case the ionic liquid fills the pores of the CQD superlattice, a large increase in the actual electrode area is expected, resulting in a much (2-5) times) higher calculated C_{el} than the value measured on bare gold. Since we do not see this effect, we can exclude a “bulk” gating using this ionic gel system. For the mobility calculations, 6 μF/cm^2 was used.

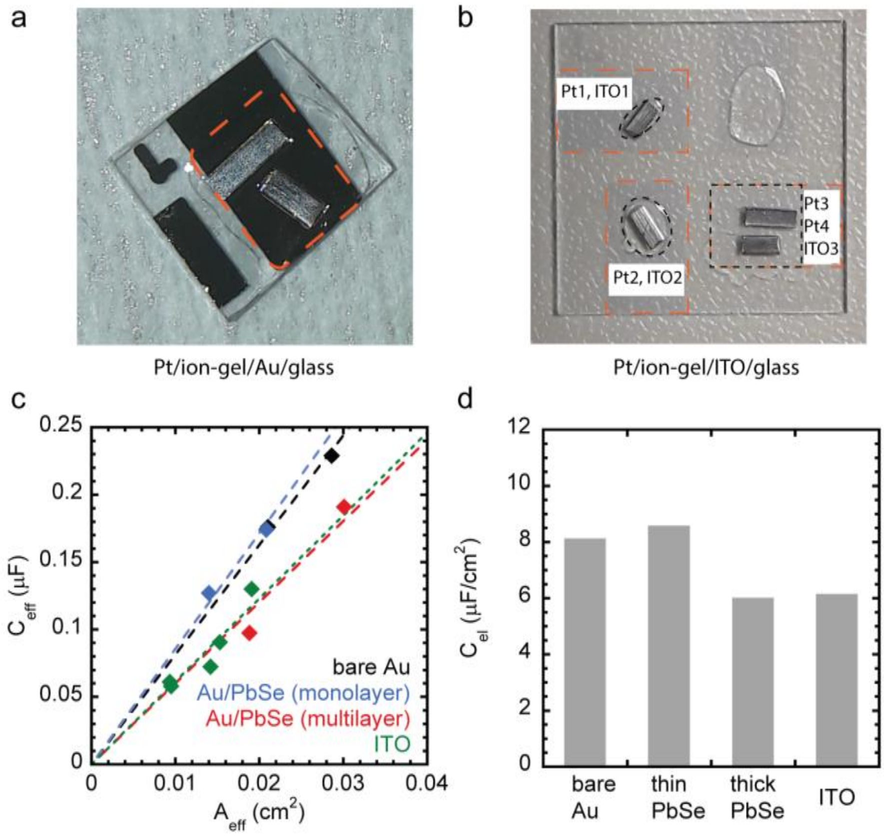

Figure S6. *The devices and data used to obtain the capacitance value for the mobility calculation; (a) ion gel sandwiched between bare Au and Pt; (b) ion gel sandwiched between ITO and Pt; (c) effective capacitance values at 63 mHz versus the effective electrode areas, and the linear fits; (d) electrolyte layer capacitance determined using different electrodes.*